JCB Article

# Detection of snRNP assembly intermediates in Cajal bodies by fluorescence resonance energy transfer

**David Staněk and Karla M. Neugebauer**

Max Planck Institute of Molecular Cell Biology and Genetics

Spliceosomal small nuclear ribonucleoprotein particles (snRNPs) are required for pre-mRNA splicing throughout the nucleoplasm, yet snRNPs also concentrate in Cajal bodies (CBs). To address a proposed role of CBs in snRNP assembly, we have used fluorescence resonance energy transfer (FRET) microscopy to investigate the subnuclear distribution of specific snRNP intermediates. Two distinct complexes containing the protein SART3 (p110), required for U4/U6 snRNP assembly, were localized: SART3•U6 snRNP and SART3•U4/U6 snRNP. These complexes segregated to different nuclear compartments, with SART3•U6 snRNPs exclusively in the nucleoplasm and SART3•U4/U6 snRNPs preferentially in CBs. Mutant cells lacking the CB-specific protein coilin and consequently lacking CBs exhibited increased nucleoplasmic levels of SART3•U4/U6 snRNP complexes. Reconstitution of CBs in these cells by expression of exogenous coilin restored accumulation of SART3•U4/U6 snRNP in CBs. Thus, while some U4/U6 snRNP assembly can occur in the nucleoplasm, these data provide evidence that SART3•U6 snRNPs form in the nucleoplasm and translocate to CBs where U4/U6 snRNP assembly occurs.

## Introduction

Nuclear bodies are nonmembrane-bound, subnuclear compartments containing specific sets of factors involved in gene expression. Proposed functions for nuclear bodies range from storage of inactive molecules or complexes to a variety of specific activities (Matera, 1999; Dundr and Misteli, 2001; Spector, 2001). Cajal bodies (CBs), were first observed ~100 yr ago by Ramon y Cajal (Gall, 2003), and contain many factors involved in transcription, RNA processing, and regulation of the cell cycle (Matera, 1999; Gall, 2000; Ogg and Lamond, 2002). Among these are the spliceosomal small nuclear RNPs (snRNPs), which are concentrated in CBs as well as distributed throughout the nucleoplasm where they play essential roles in splicing (Carmo-Fonseca et al., 1991, 1992; Matera and Ward, 1993; Neugebauer, 2002). Although specific sets of factors involved in RNA processing are concentrated in CBs, the role of CBs has for a long time been mysterious. This is because many of the complexes localized to CBs, such as snRNPs and small nucleolar RNPs (snoRNPs), participate in many reactions pertaining to multiple steps in their own maturation as well as their final activities in splicing and ribosomal RNA processing. For example, posttranscriptional modifications of both snoRNAs and snRNAs likely occur in CBs (Darzacq et al., 2002; Verheggen et al., 2002; Jady et al., 2003). Consistent with this, both snoRNPs and snRNPs transit through the CB before accumulating in nucleoli or the nucleoplasm, respectively (Narayanan et al., 1999; Sleeman and Lamond, 1999; Sleeman et al., 2001). However, the fact that snRNP accumulation in CBs is dependent on transcription and splicing suggests additional functions for CBs, such as the assembly of snRNP complexes and their regeneration after splicing (Carmo-Fonseca et al., 1992; Stanek et al., 2003). Nevertheless, the role of CBs in specific steps of snRNP assembly has not been demonstrated.

The assembly of U4/U6 spliceosomal snRNPs involves the annealing of the U4 and U6 snRNAs and stepwise assembly of U4/U6 snRNP specific proteins; subsequently, the U4/U6 snRNP associates with the U5 snRNP to produce the U4/U6•U5 tri-snRNP that is active in splicing (Will and Lührmann, 2001). During splicing, snRNPs undergo extensive structural rearrangement; in particular, the tri-snRNP disassembles and U4/U6 snRNAs unwind (Staley and Guthrie, 1998). Thus, if disassembled snRNPs participate in subsequent rounds of splicing, the U4/U6 snRNP and the U4/U6•U5

The online version of this article contains supplemental material.

Address correspondence to K.M. Neugebauer, Pfotenhauerstrasse 108, 01307 Dresden, Germany. Tel.: (49) 351-210 2589. Fax: (49) 351-210 1209. email: neugebau@mpi-cbg.de

Key words: Cajal body; snRNP; pre-mRNA splicing; coilin; FRET

Abbreviations used in this paper: CB, Cajal body; CFP, cyan fluorescent protein; FRET, fluorescence resonance energy transfer; MEF, mouse embryonic fibroblast; PA-GFP, photoactivatable green fluorescent protein; snoRNP, small nucleolar ribonucleoprotein particle; snRNA, small nuclear RNA; snRNP, small nuclear ribonucleoprotein particle.

© The Rockefeller University Press, 0021-9525/2004/09/1015/11 $8.00

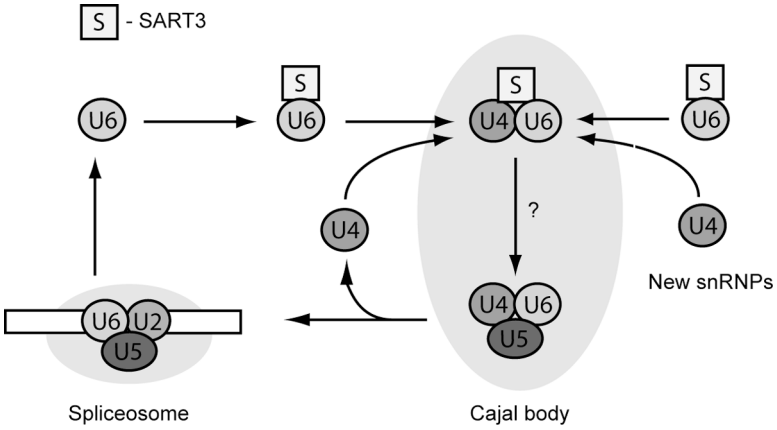


Figure 1. **Model of U4/U6 snRNP assembly in Cajal bodies.** SART3 interacts with newly synthesized U6 snRNP or with the U6 snRNP released after splicing in the nucleoplasm. The complex is then transported to Cajal bodies where formation of the U4/U6 snRNP occurs. SART3 disassociates from the U4/U6 snRNP as the U4/U6•U5 tri-snRNP complex is formed (also potentially in CBs). During formation of the active spliceosome, the tri-snRNP disassembles; U5 and U6 snRNPs play an essential role during splicing while the U4 snRNP leaves the spliceosome.

tri-snRNP have to be reassembled (Fig. 1). In yeast, U4/U6 snRNA annealing is promoted by Prp24p and the U6-associated LSm proteins, and the interaction between the Prp24p COOH-terminal domain CT-10 and LSm proteins is important for the U4/U6 snRNP assembly (Mayes et al., 1999; Raghunathan and Guthrie, 1998; Rader and Guthrie, 2002). Similarly, the human LSm proteins were shown to promote annealing of in vitro–synthesized U4 and U6 snRNAs (Achsel et al., 1999). Recently, SART3 (also named p110) was shown to be the human homologue of yeast Prp24p (Bell et al., 2002; Rader and Guthrie, 2002). SART3 was shown to bind directly to the U6 snRNA and to promote U4/U6 snRNP assembly in nuclear extracts (Bell et al., 2002). Given their demonstrated functions in vitro, and because Prp24p binds to LSm proteins, it is likely that SART3 and LSm proteins act synergistically to promote U4/U6 snRNP assembly. In contrast to the LSm proteins, however, SART3 associates exclusively with U6 and U4/U6 snRNPs and is not present in the U4/U6•U5 tri-snRNP (Bell et al., 2002). Therefore, SART3 can be used as a marker for specific steps in U4/U6 snRNP assembly.

SART3 is present in the nucleoplasm and concentrated in CBs, suggesting that steps in U4/U6 snRNP assembly occur in both compartments (Stanek et al., 2003). SART3, like snRNPs in general (Carmo-Fonseca et al., 1992), was depleted from CBs when transcription and splicing was inhibited, suggesting that SART3 in CBs may support U4/U6 reassembly after splicing. Moreover, expression of a truncated version of SART3 lacking the COOH terminus inhibited accumulation of the U6 snRNP in CBs. Based on these results, we proposed a model in which nucleoplasmic SART3 is bound to the U6 snRNP, the SART3•U6 snRNP complex translocates to CBs, and U4/U6 snRNP assembly occurs in CBs (Stanek et al., 2003). In this study, we have tested this hypothesis by determining the subnuclear location of both SART3•U6 snRNP and SART3•U4/U6 snRNP complexes, using fluorescence energy resonance transfer (FRET). We have found that SART3 interacts with the U6 snRNP proteins specifically in the nucleoplasm and with the U4/U6 snRNP proteins preferentially in CBs. Moreover, disruption of CBs lead to an increased concentration of SART3•U4/U6 snRNP intermediates in the nucleoplasm supporting a role for CBs in U4/U6 snRNP assembly.

## Results

### Coilin–coilin interaction measured by FRET

To establish a robust and specific FRET assay for CBs and the nucleoplasm, we first examined a predicted protein–protein interaction. The CB protein coilin (Raska et al., 1991) has been shown previously to bind to itself in yeast 2-hybrid and in vitro binding assays (Hebert and Matera, 2000). We tagged the coilin $NH_2$ terminus or COOH terminus with either CFP or YFP and coexpressed pairs of tagged variants in HeLa cells (Fig. 2). Note that in the following text, the position of CFP or YFP in the names of the constructs reflects tagging of the COOH or $NH_2$ terminus of the protein (i.e., CFP–coilin is tagged at the $NH_2$ terminus). FRET signals between coilin–coilin pairs were measured using confocal microscopy by the acceptor photobleaching method (Bastiaens et al., 1996; Karpova et al., 2003). FRET is detected as an increase of the donor (CFP) fluorescence after acceptor (YFP) photodestruction. First, FRET detection of the coilin–CFP/coilin–YFP pair was examined. Coilin tagged at the COOH terminus accumulated at numerous CBs with little fluorescence signal detected in the nucleoplasm (Hebert and Matera, 2000). The apparent FRET efficiencies were measured in chosen CBs (38.2 ± 2.0%), whereas the unbleached CBs served as negative controls (Fig. 2 C). Next, FRET efficiencies for CFP–coilin/YFP–coilin was measured. $NH_2$ terminally tagged coilin was detectable in the nucleoplasm and concentrated in CBs (Hebert and Matera, 2000). Robust FRET for these pairs was detected both in the nucleoplasm (39.3 ± 1.3%) and in CBs (41.2 ± 0.0%; Fig. 2 C). These results indicate that coilin proteins interact with each other in vivo both in the nucleoplasm and in CBs and that the FRET assay is able to reveal this interaction in both compartments.

Surprisingly, very low FRET efficiencies were measured both in CBs (2.8 ± 2.4%) and in the nucleoplasm (3.1 ± 0.4%) when the coilin–CFP/YFP–coilin pair was examined (Fig. 2 C). The lack of FRET between these pairs likely reflects an increased distance between donor and acceptor chromophores; the Förster radius (the distance between chromophores when the FRET efficiency is 50%) for YFP–CFP pairs is ~5 nm (Siegel et al., 2000). The other possibility is that the donor and acceptor are still in close proximity but their orientation is not favorable to produce a high FRET signal. Although both coilin–CFP and YFP–coilin ac-

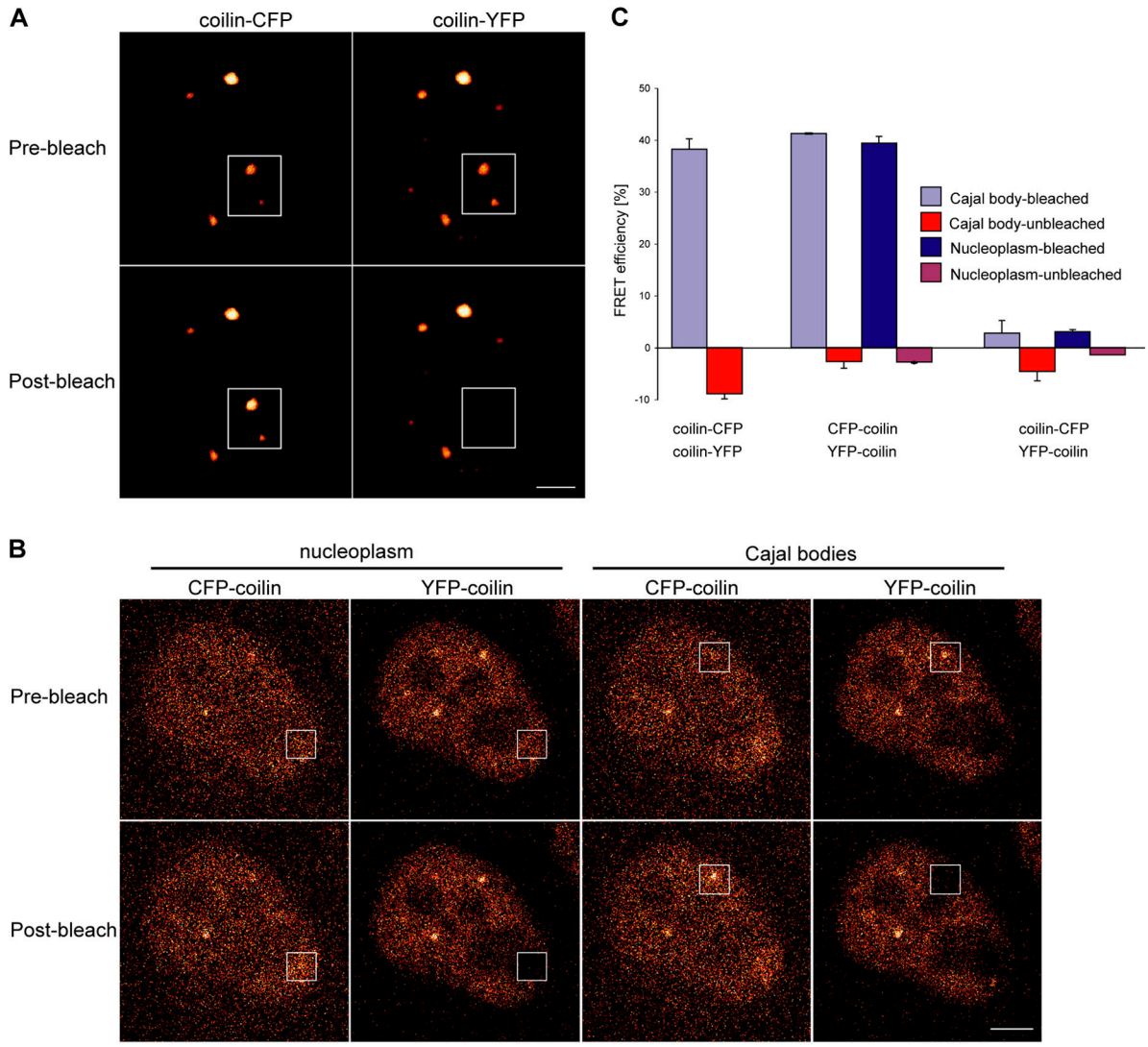


Figure 2. **FRET detection in CBs using coilin.** HeLa cells were cotransfected with (A) coilin–CFP and coilin–YFP or (B) CFP–coilin and YFP–coilin. Cells were fixed after 24 h and FRET efficiencies were measured by acceptor photobleaching in CBs (A) and in the nucleoplasm and CB (B). Unbleached areas in the nucleoplasm and unbleached CBs were used as a negative control. (C) Plot of FRET efficiencies (average of means of two independent experiments ± SEM) between coilin–coilin pairs. FRET efficiencies were measured in the bleached area within the nucleoplasm (the white box). In the case of CBs, FRET efficiencies were measured in the area of the CB only. FRET efficiency was calculated from CFP fluorescence before and after bleaching: $FRET_{efficiency}$ [%] = $(CFP_{after} - CFP_{before}) \times 100/CFP_{after}$. Very low levels of coilin–CFP/coilin–YFP pair in the nucleoplasm did not allow a FRET analysis in this compartment. The decrease of CFP fluorescence in unbleached CBs is due to bleaching during CFP detection. Bars, 5 μm.

cumulate in the same structures and coilin self-interaction is necessary for CB localization (Hebert and Matera, 2000), we cannot exclude the formal possibility that coilin molecules tagged at opposite termini do not self-interact. Importantly, the lack of FRET between these pairs indicates the specificity of the FRET observed for YFP–coilin/CFP–coilin and coilin–YFP/coilin–CFP described above and that concentration of the donor and acceptor in CBs does not lead to artificially high FRET signals.

## SART3 preferentially interacts with the U4/U6 snRNP proteins in CBs

Each snRNP contains one or more snRNAs associated with seven conserved Sm proteins (LSm in the case of the U6 snRNP) plus proteins specific for each snRNP (for review see Will and Lührmann, 2001). Biochemical studies have identified five U4/U6 snRNP proteins: 15.5K/NHPX, 61K, hPrp3 (90K), hPrp4 (60K), and USA-Cyp (20K) (Horowitz et al., 1997; Lauber et al., 1997; Nottrott et al., 1999; Makarova et al., 2002). The hPrp3 and hPrp4 proteins form, together with USA–Cyp, a stable complex that interacts with U4/U6 snRNA duplex but not with free U4 or U6 snRNAs (Nottrott et al., 2002). The 61K protein binds directly to the U4 snRNA independent of this complex (Nottrott et al., 2002). To localize the transient complex between SART3 and the U4/U6 snRNP, we tagged three U4/U6 snRNP-specific proteins, hPrp3, hPrp4, and 61K, with CFP or YFP. Western blot analysis revealed that ratios of fluorescently tagged proteins to their endogenous counterparts were 0.25 for 61K, 0.79 for hPrp4 and 2.9 for SART3 (see Fig. S1).

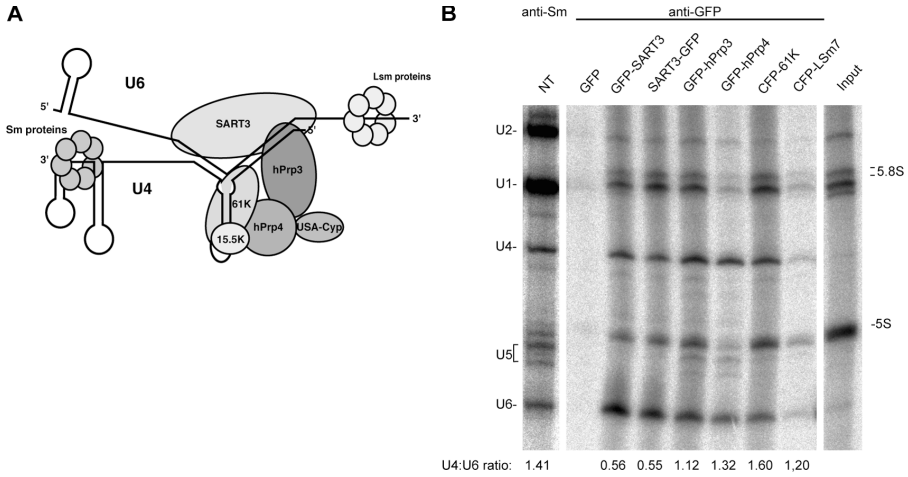


Figure 3. **Fluorescently tagged proteins assemble into snRNPs.** (A) Model of the SART3•U4/U6 snRNP complex. (B) HeLa cells were transfected with SART3, hPrp3, hPrp4, 61K, or LSm7 that have been tagged fluorescently. Total RNA was metabolically label by [$^{32}$P]orthophosphate and snRNAs were immunoprecipitated by the anti-Sm antibody (anti-Sm) or anti-GFP antibodies (anti-GFP), which cross-reacts with CFP. The anti-Sm antibody precipitated all major snRNAs, anti-GFP antibodies precipitated preferentially U4 and U6 snRNAs. Positions of snRNAs are indicated on the left and 5.8S and 5S rRNAs on the right. The 5.8S rRNAs (migrating as a doublet slightly above U1 snRNA) and 5S rRNA (migrating as a single band above U5 snRNAs) were common contaminants in our immunoprecipitations but were for unknown reasons underrepresented in GFP only controls. NT, nontransfected control.

To determine whether the tagged U4/U6 snRNP proteins and SART3 are able to assemble into U4/U6 snRNPs, fluorescently tagged proteins were transiently expressed in HeLa cells and cellular RNA was metabolically labeled with [$^{32}$P]orthophosphate. Assembled snRNPs were detected by immunoprecipitation with anti-GFP antibodies and coprecipitated snRNAs were analyzed by gel electrophoresis and autoradiography (Fig. 3 B). As a positive control, the anti-Sm antibody precipitated all major snRNAs; the relative abundance of U1, U2, U4, U5, and U6 snRNAs immunoprecipitated by anti-Sm antibodies was unaffected by transfection with any of the expression constructs (unpublished data). The anti-GFP antibodies precipitated preferentially the U4 and U6 snRNAs, indicating that the fluorescent protein tags did not interfere with U4/U6 snRNP assembly.

If U4/U6 snRNP assembly occurs in CBs, the transient SART3•U4/U6 snRNP complex should be detected preferentially in CBs (Fig. 1). To map the interaction of SART3 with U4/U6 snRNPs in situ, CFP-hPrp3, CFP-hPrp4, and CFP-61K were transiently expressed in HeLa cells. Each fluorescently tagged U4/U6 snRNP protein was detected both throughout the nucleoplasm as well as in CBs (Figs. 4 and 5; and unpublished data). No changes in CB number (~2.5/nuclei) were observed in cells expressing low or medium amounts of fluorescently tagged proteins. Cells expressing high amounts of exogenous proteins accumulated these proteins in number of bright "speckles" and nucleoli and were excluded from FRET analysis. Upon cotransfection of these constructs with YFP-SART3, FRET efficiencies between individual pairs were measured in the nucleoplasm and in a single CB within the same cell (Fig. 4). For all three pairs, FRET efficiencies were three to five times higher in CBs than in the nucleoplasm (Fig. 4 B). Several control experiments indicate the specificity of the FRET signal in CBs. First, two pairs, CFP–hPrp3/YFP–hPrp4 (Fig. 4 B) and coilin–coilin (Fig. 2), showed similar FRET efficiencies in the nucleoplasm and CBs, independent of the differential concentration of individual components in the CB compared with the nucleoplasm. Second, two unrelated CB components, fibrillarin and SART3, exhibited only 4.9 ± 0.5% FRET in CBs (Fig. 4 B). Third, 2.5 times less FRET was measured in CBs when CFP–hPrp3 was coexpressed with SART3 tagged instead at the COOH terminus (Fig. 4 B, SART3–YFP); similar results were obtained with CFP–61K and CFP–hPrp4 (unpublished data). Taken together, these data indicate that transient SART3•U4/U6 snRNP complexes are preferentially located in CBs.

These observations indicate that either U4/U6 snRNP assembly takes place in CBs and/or that U4/U6 snRNPs assembled in the nucleoplasm are transported to CBs. To distinguish between these two possibilities we used a mutant of SART3 lacking the COOH-terminal domains. We showed previously that this GFP-tagged protein (ΔCT10ΔRRM) is targeted to CBs via its $NH_2$-terminal HAT domain and reduces endogenous full-length SART3 concentration in CBs to nucleoplasmic levels (Stanek et al., 2003). Moreover, expression of this mutant reduces significantly the concentration of LSm proteins in CBs (Stanek et al., 2003), indicating that U6 snRNP concentration in CBs is dependent on full-length SART3. If SART3•U4/U6 snRNP intermediates formed in the nucleoplasm translocated subsequently to

Table I. **Concentration of the U4 snRNP in CBs is not changed upon expression of mutant SART3 (ΔCT10ΔRRM)**

| Expressed construct | Ratio of fluorescent intensities (CB/nuc.) ± SD (*n*)[a] | | |
|---|---|---|---|
| | LSm4 (U6)[b] | U4 snRNA | 61K |
| None | 1.82 ± 0.51 (124) | 1.55 ± 0.27 (88) | 1.71± 0.44 (70) |
| SART3–GFP | 1.58 ± 0.40 (130) ($P = 0.0011$)[c] | 1.64 ± 0.47 (65) ($P = 0.30$)[c] | 1.89 ± 0.53 (53) ($P = 0.079$)[c] |
| ΔCT10ΔRRM–GFP | 1.28 ± 0.27 (157) ($P \ll 10^{-10}$)[c] | 1.79 ± 0.42 (112) ($P = 0.0007$)[c] | 1.72± 0.49 (77) ($P = 0.90$)[c] |

[a]Ratio of average fluorescent intensity/pixel in CB and the nucleoplasm (nuc.); *n* = number of CBs evaluated.
[b]Data taken from Stanek et al. (2003).
[c]P values determined from the *t* test comparing fluorescent intensity ratios from the experimental data sets versus control ratios (shown in "None" row).

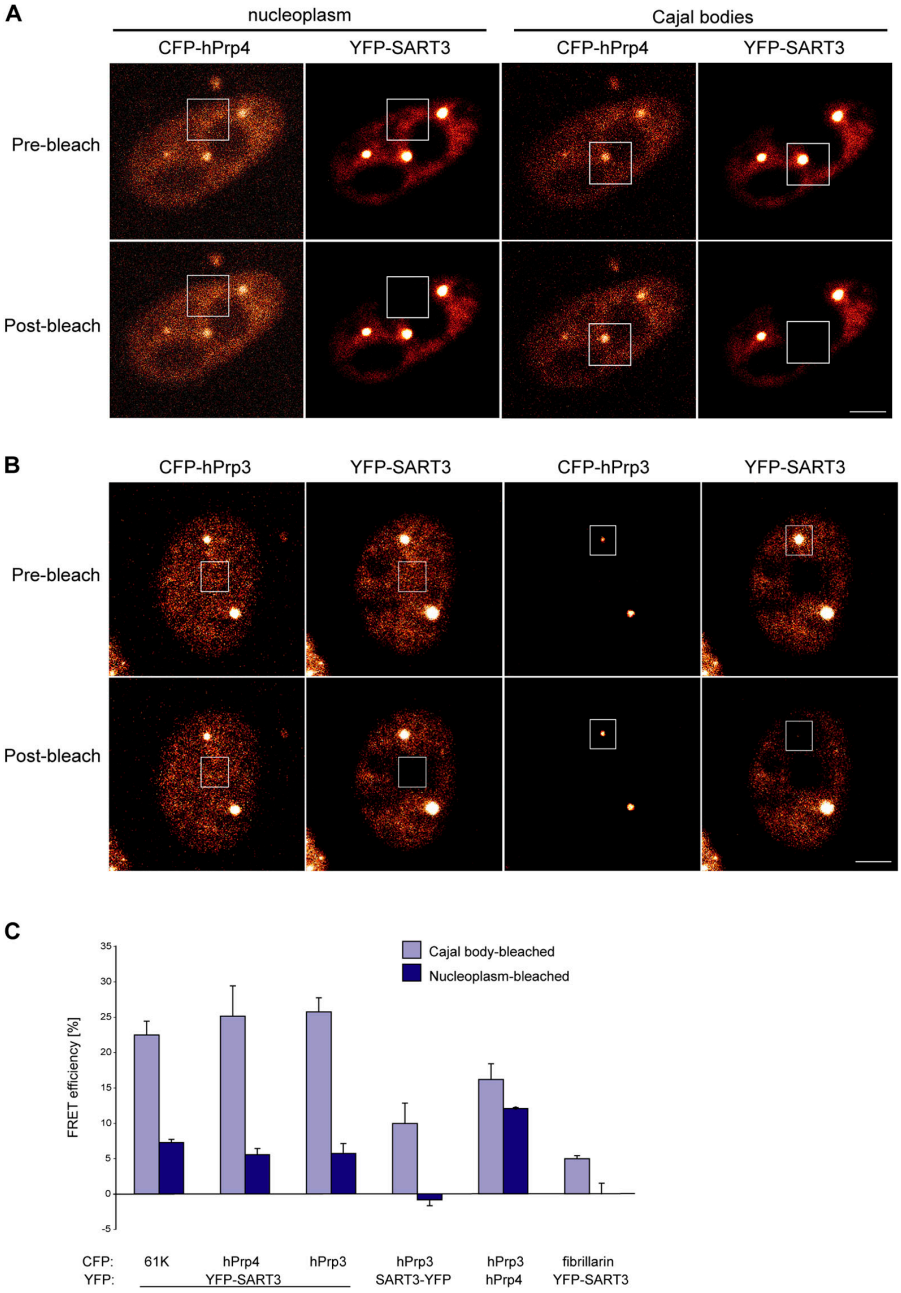


Figure 4. **SART3 preferentially associates with the U4/U6 snRNP proteins in CBs.** (A and B) HeLa cells were cotransfected with YFP–SART3 and either (A) CFP–hPrp4 or (B) CFP–hPrp3. FRET was subsequently measured in the nucleoplasm and in CBs within the same cell by acceptor photobleaching. (C) Plot of averages of means from three independent experiments between SART3 and the U4/U6 snRNP proteins 61K, hPrp3, or hPrp4. FRET efficiencies between YFP–SART3 and the U4/U6 snRNP proteins were, in all cases, three to five times higher in CBs than in the nucleoplasm. hPrp3 revealed 2.5 times lower FRET signal in CBs when coexpressed with SART3 tagged at the COOH terminus (SART3–YFP). As controls, FRET efficiencies were measured in the nucleoplasm and CBs of cells coexpressing either CFP–hPrp3/YFP–hPrp4, which form a stable complex or fibrillarin–CFP/YFP–SART3, which both localize to CBs but no interaction has been identified between them (average of two independent experiments). Bars, 5 μm.

CBs, a similar decrease in U4 snRNP CB localization would be expected. After expression of a GFP version of the ΔCT10ΔRRM mutant in HeLa cells, the U4 snRNA was detected by in situ hybridization and 61K protein by immunocytochemistry. Levels of both markers in CBs were not significantly decreased, compared with the control (Table I), indicating that the U4 snRNP concentrates in CBs independently of SART3 or the U6 snRNP. These data are consistent with the hypothesis that SART3•U6 snRNPs meet U4 in the CB where U4/U6 snRNP assembly occurs.

### SART3–U4/U6 snRNP interaction in cells lacking CBs

Our FRET data indicate that SART3•U4/U6 snRNP complexes are preferentially concentrated in CBs. If true, then disruption of CBs may lead to an elevated concentration of SART3•U4/U6 snRNP complexes in the nucleoplasm. To test this hypothesis, we compared FRET between YFP–SART3 and CFP–61K in normal mouse cells (MEF $26^{coilin+/+}$) and in mouse cells lacking functional coilin (MEF $42^{coilin-/-}$; Tucker et al., 2001). MEF $42^{coilin-/-}$ cells do not contain classical CBs, and SART3 and snRNPs are distributed throughout the nucleoplasm with no obvious concentration in any nuclear structure (Tucker et al., 2001; Stanek et al., 2003). In MEF $42^{coilin-/-}$ cell nuclei, CFP–61K was, like SART3 and snRNPs, distributed throughout the nucleoplasm (Fig. 5 A). In these cells, the nucleoplasmic FRET efficiency between YFP–SART3 and CFP–61K was 32.5 ± 1.6%, comparable with the FRET signal in CBs of coilin positive fibroblasts (Fig. 5 B). These data also indicate that coilin is not necessary for SART3 association with the U4/U6 snRNP.

In MEF $42^{coilin-/-}$ cells, CBs were successfully restored by expression of mouse coilin tagged with photoactivatable

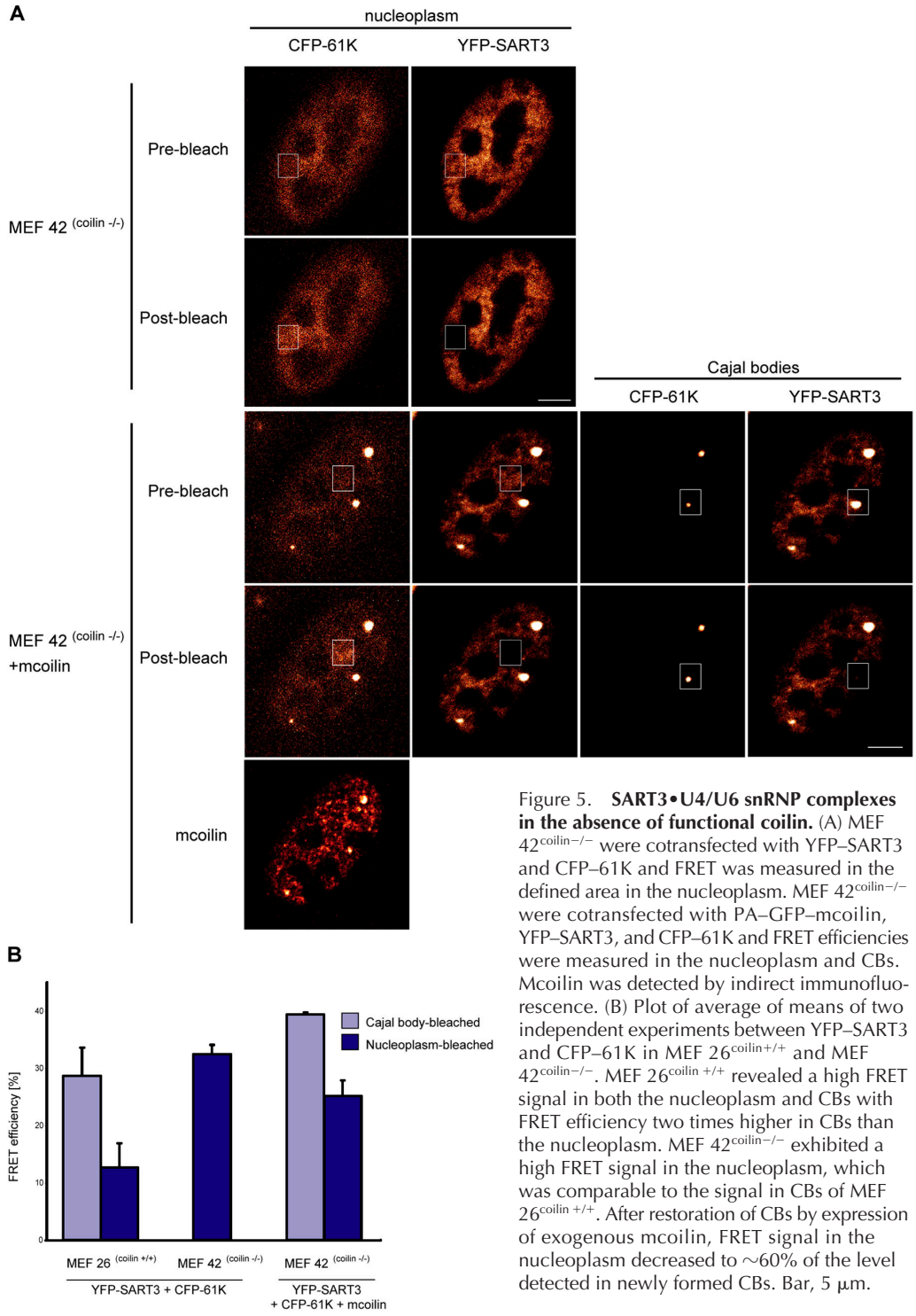


Figure 5. **SART3•U4/U6 snRNP complexes in the absence of functional coilin.** (A) MEF $42^{coilin-/-}$ were cotransfected with YFP–SART3 and CFP–61K and FRET was measured in the defined area in the nucleoplasm. MEF $42^{coilin-/-}$ were cotransfected with PA–GFP–mcoilin, YFP–SART3, and CFP–61K and FRET efficiencies were measured in the nucleoplasm and CBs. Mcoilin was detected by indirect immunofluorescence. (B) Plot of average of means of two independent experiments between YFP–SART3 and CFP–61K in MEF $26^{coilin+/+}$ and MEF $42^{coilin-/-}$. MEF $26^{coilin+/+}$ revealed a high FRET signal in both the nucleoplasm and CBs with FRET efficiency two times higher in CBs than the nucleoplasm. MEF $42^{coilin-/-}$ exhibited a high FRET signal in the nucleoplasm, which was comparable to the signal in CBs of MEF $26^{coilin+/+}$. After restoration of CBs by expression of exogenous mcoilin, FRET signal in the nucleoplasm decreased to ~60% of the level detected in newly formed CBs. Bar, 5 μm.

GFP (PA–GFP). If not activated by short wavelength laser, PA–GFP does not emit fluorescence in visible spectra (Patterson and Lippincott-Schwartz, 2002) and does not affect FRET measurements (unpublished data). When coexpressed with PA–GFP–mcoilin, YFP–SART3, and CFP–61K were distributed throughout the nucleoplasm and concentrated in the reconstituted CBs (Fig. 5 A). FRET efficiencies in the nucleoplasm decreased to 25.2 ± 2.7% whereas FRET in CBs increased to 39.4 ± 0.4%. These data indicate that CBs are not strictly required for snRNP assembly but, when CBs are present, they concentrate snRNP assembly intermediates.

## SART3 interacts with U6 snRNP LSm proteins in the nucleoplasm

We next mapped the interaction of SART3 with U6 snRNP proteins. As a first step toward localizing SART3•U6 snRNP complexes by FRET, SART3–CFP was coexpressed with YFP-tagged components of the U6 snRNP. Six of the LSm proteins (LSm2, -3, -4, -6, -7, and -8), which assemble as a

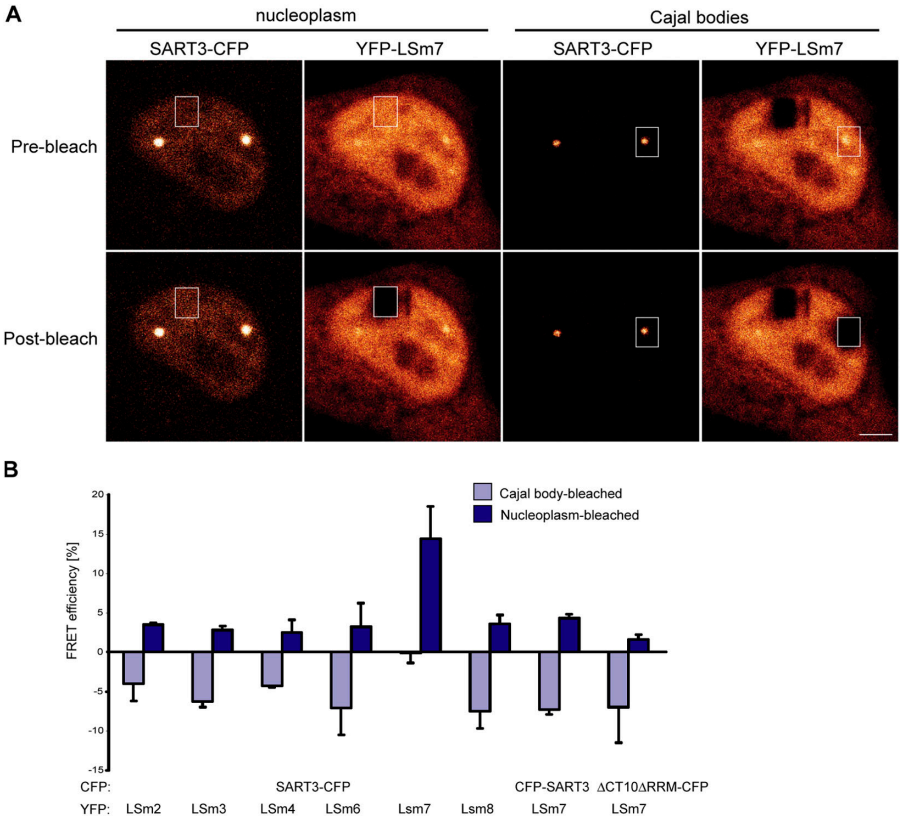


Figure 6. **SART3 interacts with U6 snRNP proteins in the nucleoplasm.** (A) HeLa cells were cotransfected with SART3–CFP and YFP–LSm7. FRET was measured by acceptor photobleaching in the nucleoplasm and in a CB within the same cell. (B) Plot of averages of means from two independent experiments between SART3 and LSm proteins. The efficiency of FRET was measured as shown in panel A and the average of means and standard error of the mean were calculated. All YFP–LSm proteins revealed a positive FRET signal with SART–CFP in the nucleoplasm but not in CBs. FRET signal in the nucleoplasm decreased four times when YFP–LSm7 was coexpressed with CFP–SART3 and nine times when coexpressed with the ΔCT10ΔRRM–CFP mutant. Bar, 5 μm.

hetero-heptamer on the 3′ end of the U6 snRNA (Achsel et al., 1999; Mayes et al., 1999), were tested individually for FRET with SART3. It was shown previously that LSm proteins expressed with fluorescence protein tags retain their ability to form the heteromeric complex (Ingelfinger et al., 2002). Moreover, fluorescently tagged SART3 and LSm7 were incorporated into U4/U6 snRNPs (Fig. 3 B). Within the cell nucleus, each YFP-tagged LSm protein was detected both in the nucleoplasm and CBs (Stanek et al., 2003; and data not shown). FRET efficiencies were measured between SART3 and LSm proteins in the nucleoplasm and in CBs within the same cell (Fig. 6 A). Interestingly, FRET efficiencies varied among the LSm proteins, with the highest FRET signals reproducibly obtained from the SART3–LSm7 pair (Fig. 6 B). However, for all tagged LSm proteins, a positive FRET signal with SART3 in the nucleoplasm was observed. Surprisingly, none of the SART3–LSm pairs produced FRET in CBs (Fig. 6 B).

To validate the observed nucleoplasmic FRET between LSm7 and SART3, specific predictions regarding the topology of SART3 with respect to LSm7 were investigated. It was shown previously that the COOH-terminal domain of Prp24p and the RRM domains of SART3 interact with LSm proteins and the U6 snRNA, respectively (Bell et al., 2002; Rader and Guthrie, 2002; Medenbach et al., 2004). To determine the specificity of the SART3–CFP/YFP–LSm7 FRET signal, YFP–LSm7 was coexpressed with the mutant of SART3 lacking the CT10 domain as well as the RRMs (ΔCT10ΔRRM–CFP). This mutant protein would not be expected to bind to the U6 snRNP alone. Indeed, nucleoplasmic FRET for this pair was ninefold reduced, compared with full-length SART3 (Fig. 6). As a second control, FRET was measured between YFP–LSm7 and SART3 tagged instead at its $NH_2$ terminus (CFP–SART3). Nucleoplasmic FRET for this pair was fourfold reduced, compared with SART3 tagged at its COOH terminus (Fig. 6 B). These data are consistent with the role of the SART3 CT10 domain in binding to LSm proteins and confirm the specificity of the FRET signals observed between SART3–CFP and YFP–LSm7. Given that all of the LSm proteins are present in the nucleoplasm as well as CBs, the observation of specific FRET between LSm7 and SART3 in the nucleoplasm indicates that configuration of SART3 and U6-specific proteins within assembly intermediates is favorable for FRET only in the nucleoplasm.

## Discussion

It has been difficult to establish the functions of nuclear bodies, because the molecules concentrated within each nuclear body are also present in the nucleoplasm; thus, the localization of particular components to nuclear bodies is not enough to suggest the sites of molecular function. Moreover, the rapid trafficking of molecules to and from nuclear bodies indicate that biochemical isolation of nuclear bodies is of limited utility for functional studies (Dundr et al., 2002, 2004). To identify particular events occurring in CBs, assays capable of localizing specific molecular activities are needed. To this end, we have studied the protein SART3, which is required for U4/U6 snRNP assembly (Bell et al., 2002). Here we have used FRET to determine the distribution of two known SART3-containing complexes (SART3•U6 sn-

RNP and SART3•U4/U6 snRNP), which transiently form before U4/U6•U5 tri-snRNP formation and splicing. Our principal finding is that these two intermediates segregate to distinct compartments of the nucleus: SART3 interacts with U6 snRNP–LSm proteins exclusively in the nucleoplasm, and SART3•U4/U6 snRNP complexes were located preferentially in CBs. Whereas U4/U6 snRNP components are enriched in CBs only twofold above nucleoplasmic levels (Table I), the SART3•U4/U6 snRNP intermediate detected by FRET is more dramatically enriched, by up to fivefold in CBs (Fig. 4). These data directly implicate the CB in spliceosomal snRNP assembly.

Because the detection of FRET between two fluorescent molecules depends strongly on their proximity (Siegel et al., 2000), this technique can provide strong evidence that two proteins interact, either directly or indirectly, within the cell. The conditions for detecting specific FRET in CBs were identified by examining the protein coilin (Fig. 2) that has been shown to bind to itself in vitro and in a yeast two-hybrid assay (Hebert and Matera, 2000). Recently, it was shown by FRET that coilin interacts with itself in CBs in living cells (Dundr et al., 2004). Using fixed samples, we show here that coilin interacts with itself both in CBs and the nucleoplasm. Moreover, coilin–coilin FRET detection was dependent on the position of the fluorescent protein tag, such that only when both partners were tagged on their $NH_2$ termini or COOH termini was FRET observed. This provides an important negative control for the possibility that FRET signals could be generated nonspecifically by the high concentration of chromophores in CBs. Interestingly, coilin–coilin interactions were detectable by FRET in both the nucleoplasm and the CB (Fig. 2). Thus, although coilin is a prominent and relatively stable component of CBs (Handwerger et al., 2003; Sleeman et al., 2003; Stanek et al., 2003; Dundr et al., 2004), its role in CB assembly must not be limited to coilin self-interaction, which can also occur in the nucleoplasm.

A similar FRET approach was used to map the subnuclear location of SART3 interactions with the U6 and U4/U6 snRNPs. In CBs, robust FRET signals were measured between SART3 and specific components of the U4/U6 snRNP, namely hPrp3, hPrp4, and 61K; to a lesser extent, these FRET signals were detected in the nucleoplasm (Figs. 4 and 5). These data likely reflect the interaction of SART3 with U4/U6 snRNP complexes rather than free proteins, because similar levels of FRET were detected between SART3 and all three proteins that assemble in step-wise fashion on the U4/U6 snRNP (Nottrott et al., 2002). This interpretation is also supported by the recent finding that the $NH_2$-terminal HAT domain of SART3 interacts directly with hPrp3 and not hPrp4 or 61K (Medenbach et al., 2004). Indeed, FRET between SART3 and the three U4/U6 snRNP proteins was observed when the fluorescent protein was placed on the $NH_2$ terminus of SART3; placement of the tag at the SART3 COOH terminus led to a significant reduction of FRET between full-length SART3 and U4/U6 snRNP-specific proteins. We cannot exclude the formal possibility that complexes in CBs undergo conformational changes more favorable for FRET; however, high FRET signals between SART3 and 61K were detected in the nucleoplasm of cells lacking coilin and CBs. Therefore, any conformational changes influencing FRET detection of the SART3•U4/U6 snRNP complex must not be coilin or CB specific. Thus, CBs are enriched in complexes of SART3 with the U4/U6 snRNP.

SART3 is also a component of the U6 snRNP, containing seven LSm proteins (LSm 2–8), which are not present in any other spliceosomal snRNP (Stevens et al., 2001; Will and Lührmann, 2001; Bell et al., 2002). Positive FRET interactions between SART3 and LSm proteins were detected exclusively in nucleoplasm (Fig. 6). Because SART3 and LSm proteins bind directly to the U6 snRNA (Achsel et al., 1999; Medenbach et al., 2004), we anticipate that the FRET observed between SART3 and LSm proteins in the nucleoplasm is representative of the pool of SART3 associated with the U6 snRNP. Interestingly, robust FRET between SART3 and LSm proteins was only detected with LSm7 (Fig. 6) even though two-hybrid studies indicate that yeast Prp24p can bind LSm2, -3, -4, -5, -7, and -8 through the CT10 domain (Rader and Guthrie, 2002). This may be due to structural constraints within the U6 snRNP and/or fluorescent tags themselves that might favor high FRET between SART3 and LSm7 only. A second possibility is that SART3, unlike yeast Prp24p, preferentially binds LSm7. Consistent with the expectation that the CT10 domain mediates interactions with LSm7, reduced FRET signals were observed when full-length SART3 was tagged on the $NH_2$ terminus and when the COOH-terminal domains of SART3 were deleted (Fig. 6). Note that SART3 and LSm proteins also bind the minor U6atac snRNA and promote assembly of the U4atac/U6atac snRNP (Damianov et al., 2004); therefore a small component of FRET measured between SART3 and LSm7 may represent this less abundant pool of intermediates.

Because SART3 is required for accumulation of U6 snRNPs in CBs (Stanek et al., 2003), detection of SART3–LSm protein interactions in the nucleoplasm was expected. Surprisingly, FRET between SART3 and LSm proteins was not observed in CBs (Fig. 6), even though both SART3 and LSm proteins were present in CBs. Because SART3 has not been detected in any U4 snRNA-containing complex lacking U6 (Bell et al., 2002), we anticipate that U6 must be present in the observed CB-specific complex (see Discussion). This finding suggests that U4/U6 snRNP assembly is accompanied by a conformational change, which is unfavorable for FRET between SART3 and LSm proteins.

The observation that the two distinct pools of SART3 (SART3•U6 snRNP and SART3•U4/U6 snRNP) are unequally distributed between nucleoplasm and CBs leads us to propose that the nucleoplasmic SART3•U6 snRNP complex translocates to CBs where U4/U6 snRNP assembly occurs. This is consistent with the previous finding that U6 snRNP accumulation in CBs is SART3-dependent (Stanek et al., 2003). An alternative is that SART3•U4/U6 snRNPs detected in CBs were assembled in the nucleoplasm and subsequently translocated to the CB. However, the reduction of U6 snRNP levels in CBs upon overexpression of the dominant negative mutant of SART3 is not accompanied by a decrease of U4 snRNA levels (Table I), suggesting that the U4 snRNA is recruited to CBs independently of the U6 snRNP and/or U4/U6 snRNP assembly, as was shown in *Xenopus*

oocytes (Gerbi et al., 2003). Thus, it is currently unknown how the U4 snRNA is targeted to CBs. These, and previous, results imply that the SART3•U6 snRNP complex meets the U4 snRNA in the CB. However, the coilin deficient situation that lacks CBs indicates that CBs are not absolutely essential for U4/U6 snRNP formation, which can also occur in the nucleoplasm. Because the U5 snRNA has been localized to CBs as well (Carmo-Fonseca et al., 1992; Matera and Ward, 1993), tri-snRNP formation may also occur in CBs and lead to the release of SART3 from the U4/U6 snRNP. This model is supported by the observation that SART3 has shorter residency time in the CB than the snRNP proteins SmB and SmD1 (Dundr et al., 2004). Taken together, these data indicate that distinct steps in snRNP assembly are compartmentalized within the cell nucleus and strongly support the role of CBs in U4/U6 snRNP assembly.

Some cells lack morphologically defined CBs, suggesting that CBs per se are not required for cell survival. Indeed, while coilin expression is required for the concentration of many CB-specific components in nuclear bodies, coilin is not strictly required for viability or for snRNA base modification (Tucker et al., 2001; Jady et al., 2003). We show here that the SART3•U4/U6 complex forms in the nucleoplasm of coilin$^{-/-}$ cells (Fig. 5), indicating that coilin is not required for complex formation and that U4/U6 snRNP assembly likely occurs in the nucleoplasm of cells lacking CBs. Moreover, complementation of the coilin deficiency in these cells through transient transfection of a coilin expression construct restored the localization of SART3•U4/U6 snRNP intermediates to CBs.

The observation that specific events in snRNP assembly are compartmentalized in cell nuclei suggests that the concentration of snRNPs in CBs may confer certain cellular advantages. More CBs are present in transformed cells and in actively dividing cells compared with quiescent cells within tissues (Boudonck et al., 1998). In neurons, CB number correlates with cell size (Pena et al., 2001). We speculate that recruitment of snRNP assembly intermediates to CBs may support high metabolic activity of cells. On the one hand, concentration of nonfunctional snRNPs in CBs may increase splicing efficiency, by sequestering them away from nucleoplasm where they might compete with active snRNPs in the splicing process. On the other hand, the concentration of inactive snRNPs in CBs might either promote efficient snRNP assembly or alternatively contribute to the accuracy of snRNP assembly in a manner analogous to SMN protein function, in which proper assembly of Sm– and LSm–protein heteroheptamers onto snRNAs is regulated (Yong et al., 2004). Indeed, CBs may self-assemble in highly active cells; in this case, CB formation would be coilin dependent and driven by high levels of splicing and/or de novo snRNP synthesis.

## Materials and methods

### Protein cloning and tagging

Cloning of GFP–SART3, GFP–ΔCT10ΔRRM mutant, LSm8–YFP, and fibrillarin–GFP was described previously (Stanek et al., 2001, 2003). The full-length SART3 and the ΔCT10ΔRRM mutant (amino acids 1–702) were cloned into EYFP–C3, ECFP–C3, EYFP–N1, and ECFP–N1 (Clontech Laboratories, Inc.) using BglII and EcoRI sites. Fibrillarin was cloned to ECFP–N1 vector using BamHI and HindIII rectriction sites. Human GFP–coilin (Hebert and Matera, 2000) and mouse GFP–coilin used previously for complementation of MEF 42$^{coilin-/-}$ (Tucker et al., 2001) were obtained from A. Greg Matera (Case Western University, Cleveland, OH). Coilin and mcoilin ORFs were amplified using Expand long template PCR system (Roche) and cloned into EYFP–N1, ECFP–N1, EYFP–C3, and ECFP–C3 in the case of human coilin and PA–GFP–C1 in the case of mcoilin using BamHI and KpnI sites. Human cDNAs of hPrp3 and hPrp4 (Horowitz et al., 1997) were obtained from David S. Horowitz (Cold Spring Harbor Laboratory, Cold Spring Harbor, NY), amplified using Expand long template PCR system and cloned into EYFP–C1 or ECFP C1 using XhoI and BamHI sites. EST clones of human 61K, LSm2–4, -6, and -7 were obtained from RZPD and ORFs were amplified by Expand long template PCR system. 61K was cloned into ECFP–C3 using EcoRI and BamHI sites, LSms were cloned into EYFP–C3 and ECFP–C3 using BglII and EcoRI sites.

### FRET measurement

HeLa cells, mouse embryonic fibroblasts 42$^{coilin-/-}$ and 26$^{coilin+/+}$ (gift of A. Greg Matera) were cultured in Dulbecco's modified Eagle medium (Invitrogen) supplemented with 10% fetal calf serum (GIBCO BRL), penicillin, and streptomycin (GIBCO BRL). Cells were transfected with fluorescent protein-tagged constructs using Fugene 6 (Roche), grown for 24–28 h and fixed in 4% PFA/Pipes for 10 min at room temperature. After rinsing with Mg–PBS (PBS supplemented with 10 mM $Mg^{2+}$) and water, cells were embedded in glycerol containing 2.5% 1,4-Diazabicyclo [2.2.2]octane (DABCO; Sigma Aldrich) as an antifade reagent. FRET was measured by acceptor photobleaching method (Bastiaens et al., 1996; Karpova et al., 2003). FRET measurement was performed on the Leica TCS SP2 confocal microscope using the FRET acceptor photobleaching protocol (Leica). The HCX PL APO 100×/1.40–0.7 oil CS and HCX PL APO 63×/1.32–0.6 oil CS objectives and Ar 20m Watt laser were used. The 454-nm laser line was used for CFP detection, the laser line 514 nm was used for detection and photobleaching of YFP. For YFP detection, laser intensity was set to 2%. YFP was bleached by three consecutive pulses using 20% laser intensity. Minimal CFP bleaching (0–2%) was observed and was not taken into account for the calculation of FRET efficiency. The gain of the photomultiplier detectors was adjusted to obtain the optimal dynamic range. The CFP fluorescence was measured before ($CFP_{before}$) and after ($CFP_{after}$) the YFP bleaching and apparent FRET efficiency calculated according to the equation $FRET_{efficiency}[\%] = (CFP_{after} - CFP_{before}) \times 100/CFP_{after}$. First, a region in the nucleoplasm was bleached and FRET efficiency measured. In the same cell, the region (of the same area as in the nucleoplasm) was then bleached around a selected CB. The efficiency of FRET was measured in CB area only. Unbleached regions of the nucleoplasm and CB of the given cell were always used as a negative control. Mean of unbleached regions were −10–0% for each pair tested. 10 cells were measured in each experiment. Standard deviations of individual experiments reflecting differences between individual cells were 20–30% of the mean. Experiments were done in duplicates or triplicates and average of means ± standard error of the mean are presented.

### Immunoprecipitation and Western blotting

HeLa cells were grown on a 15-cm Petri dish, transfected with either GFP, GFP–SART3, SART3–GFP, GFP–hPrp3, GFP–hPrp4, CFP–61K, and CFP–LSm7, and grown for 28 h. Cells were labeled before harvesting for 12 h with [$^{32}$P]orthophosphate (100 μCi/plate). Cells were placed on ice, washed three times with ice cold Mg–PBS, scraped in NET-2 buffer (50 mM TRIS-Cl, pH 7.5, 150 mM NaCl, 0.05% Nonidet P-40) supplemented with complete mix of protease inhibitors (Roche) and sonicated three times for 30 s on ice. The cell extract was centrifuged at 13,000 rpm and supernatant was incubated either with a monoclonal anti-Sm antibody (Y12) in the case of nontransfected cells or with goat anti–GFP antibodies (raised against bacterially expressed full-length EGFP and obtained from David Drechsel, MPI-CBG, Dresden, Germany) for 4 h at 4°C. RNA was extracted using phenol/chloroform, resolved on denaturing polyacrylamide gel, and snRNAs detected by Phosphoimager FLA-3000 film (Fuji).

Alternatively, cells expressing YFP–SART3, CFP–61K, or YFP–hPrp4 were extracted in NET-2 buffer and 10 μg of total protein were resolved on 7.5% polyacrylamide gel and proteins detected by Western blotting. Polyclonal antisera specific for the COOH terminus of SART3 (Stanek et al., 2003), 61K (Makarova et al., 2002), and anti-hPrp4 (Nottrott et al., 2002) were used in this analysis.

### In situ hybridization

Digoxigenin-labeled probes directed against human U4 snRNA were obtained by PCR as described previously (Bell et al., 2002) using pSPU4b

(Black and Pinto, 1989) as a template. HeLa cells were transfected with SART3–GFP or ΔCT10ΔRRM–GFP using Fugene 6, and after 24 h fixed in 4% PFA for 10 min. Cells were permeabilized with 0.5% Triton X-100 for 5 min and in the case of untransfected control incubated with anti-coilin antibody (5P10; Almeida et al., 1998) provided by M. Carmo-Fonseca (University of Lisbon, Lisbon, Portugal) followed by treatment with anti–mouse antibody conjugated with FITC (Jackson ImmunoResearch Laboratories). Cells were then fixed in 4% PFA for 5 min, quenched for 5 min in 0.1 M glycine/0.2 M Tris, pH 7.4, and incubated with dig-labeled anti-U4 probe in 2× SSC/50% formamide/10% dextran sulfate/1% BSA for 60 min at 37°C. After washing in 2× SSC/50% formamide, 2× SSC, and 1× SSC, the probe was detected by anti-digoxygenin antibody conjugated with TRITC (Jackson ImmunoResearch Laboratories). Images were collected using the DeltaVision microscope system (Applied Precision) coupled with Olympus IX70 microscope. Stacks of 25 optical sections with z-step set to 200 nm were collected per sample and subjected to mathematical deconvolution (SoftWorx; Applied Precision).

### Indirect immunofluorescence

HeLa cells were transfected with SART3–GFP or ΔCT10ΔRRM–GFP using Fugene 6. After 24 h the cells were fixed in 4% PFA (Sigma-Aldrich) for 10 min, permeabilized for 5 min with 0.2% Triton X-100 (Sigma-Aldrich), and incubated with anti-61K antibody (Makarova et al., 2002; gift of R. Lührmann, MPI, Göttingen, Germany) and in the case of untransfected control also with monoclonal antibody anti-coilin (5P10). Secondary anti–rabbit antibodies conjugated with TRITC and anti–mouse antibodies conjugated with FITC (Jackson ImmunoResearch Laboratories) were used. Images were collected using DeltaVision microscope system as described above. MEF $42^{coilin-/-}$ cotransfected with PA–GFP–mcoilin, CFP–61K, and YFP–SART3 were fixed and permeabilized as above and mcoilin was detected by rabbit anti-coilin antibodies (R288; gift of E.K.L. Chan, University of Florida, Gainesville, FL); Andrade et al., 1991) and anti–rabbit antibodies conjugated with Cy5 (Jackson ImmunoResearch Laboratories). Cy5 was detected on Leica TCS SP2 confocal microscope after FRET measurement.

### Measurement of fluorescence intensities

Fluorescence intensities were quantified with SoftWorx software using deconvolved images (see In situ hybridization) as described previously (Stanek et al., 2003). The optical sections were merged and the intensities in random regions of the nucleoplasm divided by the region area was taken as the value to which the intensities within the CBs were compared. CB area was defined by SART3–EGFP constructs or by coilin labeling; intensities of U4 snRNA or 61K protein were measured within the CB and divided by the CB area. Data were collected from ~20 cells.

### Online supplemental material

Figure S1 shows Western blot analysis of fluorescently tagged proteins. HeLa cells were transfected with 61K, hPrp4, or SART3 proteins tagged fluorescently and cell extracts were made after 24 h. Proteins were resolved by SDS-PAGE, transfered to a nitrocellulose membrane, and tagged proteins as well as their endogenous counterparts were detected by appropriate antibodies: (lanes 1 and 2) anti-61K; (lanes 3 and 4) anti-hPrp4; and (lanes 5 and 6) anti-SART3. Extract from nontransfected cells (NT; lines 1, 3, and 5) was used as a negative control. Intensities of protein bands were determined by TotalLab. Online supplemental materials are available at http://www.jcb.org/cgi/content/full/jcb.200405160/DC1.

We would like to thank D. Horowitz, A.G. Matera, R. Lührmann, M. Carmo-Fonseca, E.K.L. Chan and D. Drechsel for reagents, J. Peychl for assistance with FRET measurements, and J.R. Swedlow and members of Neugebauer lab (especially K. Kotovic) for helpful discussions. We thank A. Bindereif and S. Rader for helpful discussion and communicating unpublished results.

This work was supported by grants from the American Cancer Society (RPG-00-110-01-MGO) and the Deutsche Forschungsgemeinschaft (NE 909/1-1) and by the Max Planck Gesellschaft.

Submitted: 27 May 2004
Accepted: 5 August 2004

**Note added in proof.** Evidence that the U4/U6 snRNP accumulates in CBs when tri-snRNP formation is inhibited was recently published (Schaffert, W., M. Hossbach, R. Heintzmann, T. Aschel, and R. Lührmann. 2004. *EMBO J.* 23:3000–3009).

## References

Achsel, T., H. Brahms, B. Kastner, A. Bachi, M. Wilm, and R. Lührmann. 1999. A doughnut-shaped heteromer of human Sm-like proteins binds to the 3′-end of U6 snRNA, thereby facilitating U4/U6 duplex formation in vitro. *EMBO J.* 18:5789–5802.

Almeida, F., R. Saffrich, W. Ansorge, and M. Carmo-Fonseca. 1998. Microinjection of anti-coilin antibodies affects the structure of coiled bodies. *J. Cell Biol.* 142:899–912.

Andrade, L.E., E.K. Chan, I. Raska, C.L. Peebles, G. Roos, and E.M. Tan. 1991. Human autoantibody to a novel protein of the nuclear coiled body: immunological characterization and cDNA cloning of p80-coilin. *J. Exp. Med.* 173:1407–1419.

Bastiaens, P.I., I.V. Majoul, P.J. Verveer, H.D. Soling, and T.M. Jovin. 1996. Imaging the intracellular trafficking and state of the AB5 quaternary structure of cholera toxin. *EMBO J.* 15:4246–4253.

Bell, M., S. Schreiner, A. Damianov, R. Reddy, and A. Bindereif. 2002. p110, a novel human U6 snRNP protein and U4/U6 snRNP recycling factor. *EMBO J.* 21:2724–2735.

Black, D.L., and A.L. Pinto. 1989. U5 small nuclear ribonucleoprotein: RNA structure analysis and ATP-dependent interaction with U4/U6. *Mol. Cell. Biol.* 9:3350–3359.

Boudonck, K., L. Dolan, and P.J. Shaw. 1998. Coiled body numbers in the Arabidopsis root epidermis are regulated by cell type, developmental stage and cell cycle parameters. *J. Cell Sci.* 111:3687–3694.

Carmo-Fonseca, M., R. Pepperkok, M.T. Carvalho, and A.I. Lamond. 1992. Transcription-dependent colocalization of the U1, U2, U4/U6, and U5 snRNPs in coiled bodies. *J. Cell Biol.* 117:1–14.

Carmo-Fonseca, M., R. Pepperkok, B.S. Sproat, W. Ansorge, M.S. Swanson, and A.I. Lamond. 1991. In vivo detection of snRNP-rich organelles in the nuclei of mammalian cells. *EMBO J.* 10:1863–1873.

Damianov, A., S. Schreiner, and A. Bindereif. 2004. Recycling of the U12-type spliceosome requires p110, a component of the U6atac snRNP. *Mol. Cell. Biol.* 24:1700–1708.

Darzacq, X., B.E. Jady, C. Verheggen, A.M. Kiss, E. Bertrand, and T. Kiss. 2002. Cajal body-specific small nuclear RNAs: a novel class of 2'-O-methylation and pseudouridylation guide RNAs. *EMBO J.* 21:2746–2756.

Dundr, M., M.D. Hebert, T.S. Karpova, D. Stanek, H. Xu, K.B. Shpargel, U.T. Meier, K.M. Neugebauer, A.G. Matera, and T. Misteli. 2004. In vivo kinetics of Cajal body components. *J. Cell Biol.* 164:831–842.

Dundr, M., U. Hoffmann-Rohrer, Q. Hu, I. Grummt, L.I. Rothblum, R.D. Phair, and T. Misteli. 2002. A kinetic framework for a mammalian RNA polymerase in vivo. *Science.* 298:1623–1626.

Dundr, M., and T. Misteli. 2001. Functional architecture in the cell nucleus. *Biochem. J.* 356:297–310.

Gall, J.G. 2000. Cajal bodies: the first 100 years. *Annu. Rev. Cell Dev. Biol.* 16: 273–300.

Gall, J.G. 2003. The centennial of the Cajal body. *Nat. Rev. Mol. Cell Biol.* 4:975–980.

Gerbi, S.A., A.V. Borovjagin, F.E. Odreman, and T.S. Lange. 2003. U4 snRNA nucleolar localization requires the NHPX/15.5-kD protein binding site but not Sm protein or U6 snRNA association. *J. Cell Biol.* 162:821–832.

Handwerger, K.E., C. Murphy, and J.G. Gall. 2003. Steady-state dynamics of Cajal body components in the Xenopus germinal vesicle. *J. Cell Biol.* 160:495–504.

Hebert, M.D., and A.G. Matera. 2000. Self-association of coilin reveals a common theme in nuclear body localization. *Mol. Biol. Cell.* 11:4159–4171.

Horowitz, D.S., R. Kobayashi, and A.R. Krainer. 1997. A new cyclophilin and the human homologues of yeast Prp3 and Prp4 form a complex associated with U4/U6 snRNPs. *RNA.* 3:1374–1387.

Ingelfinger, D., D.J. Arndt-Jovin, R. Lührmann, and T. Achsel. 2002. The human LSm1-7 proteins colocalize with the mRNA-degrading enzymes Dcp1/2 and Xrnl in distinct cytoplasmic foci. *RNA.* 8:1489–1501.

Jady, B.E., X. Darzacq, K.E. Tucker, A.G. Matera, E. Bertrand, and T. Kiss. 2003. Modification of Sm small nuclear RNAs occurs in the nucleoplasmic Cajal body following import from the cytoplasm. *EMBO J.* 22:1878–1888.

Karpova, T.S., C.T. Baumann, L. He, X. Wu, A. Grammer, P. Lipsky, G.L. Hager, and J.G. McNally. 2003. Fluorescence resonance energy transfer from cyan to yellow fluorescent protein detected by acceptor photobleaching using confocal microscopy and a single laser. *J. Microsc.* 209:56–70.

Lauber, J., G. Plessel, S. Prehn, C.L. Will, P. Fabrizio, K. Groning, W.S. Lane, and R. Lührmann. 1997. The human U4/U6 snRNP contains 60 and 90kD proteins that are structurally homologous to the yeast splicing factors Prp4p and Prp3p. *RNA.* 3:926–941.

Makarova, O.V., E.M. Makarov, S. Liu, H.P. Vornlocher, and R. Lührmann. 2002. Protein 61K, encoded by a gene (PRPF31) linked to autosomal dominant retinitis pigmentosa, is required for U4/U6center dotU5 tri-snRNP formation and pre-mRNA splicing. *EMBO J.* 21:1148–1157.

Matera, A.G. 1999. Nuclear bodies: multifaceted subdomains of the interchromatin space. *Trends Cell Biol.* 9:302–309.

Matera, A.G., and D.C. Ward. 1993. Nucleoplasmic organization of small nuclear ribonucleoproteins in cultured human cells. *J. Cell Biol.* 121:715–727.

Mayes, A.E., L. Verdone, P. Legrain, and J.D. Beggs. 1999. Characterization of Sm-like proteins in yeast and their association with U6 snRNA. *EMBO J.* 18:4321–4331.

Medenbach, S. Schreiner, S. Liu, R. Lührmann, and A. Bindereif. 2004. Human U4/U6 snRNP recycling factor p110: mutational analysis reveals function of TPR domain in recycling. *Mol. Cell. Biol.* In press.

Narayanan, A., W. Speckmann, R. Terns, and M.P. Terns. 1999. Role of the box C/D motif in localization of small nucleolar RNAs to coiled bodies and nucleoli. *Mol. Biol. Cell.* 10:2131–2147.

Neugebauer, K.M. 2002. On the importance of being co-transcriptional. *J. Cell Sci.* 115:3865–3871.

Nottrott, S., K. Hartmuth, P. Fabrizio, H. Urlaub, I. Vidovic, R. Ficner, and R. Lührmann. 1999. Functional interaction of a novel 15.5kD [U4/U6.U5] tri-snRNP protein with the 5′ stem-loop of U4 snRNA. *EMBO J.* 18: 6119–6133.

Nottrott, S., H. Urlaub, and R. Lührmann. 2002. Hierarchical, clustered protein interactions with U4/U6 snRNA: a biochemical role for U4/U6 proteins. *EMBO J.* 21:5527–5538.

Ogg, S.C., and A.I. Lamond. 2002. Cajal bodies and coilin–moving towards function. *J. Cell Biol.* 159:17–21.

Patterson, G.H., and J. Lippincott-Schwartz. 2002. A photoactivatable GFP for selective photolabeling of proteins and cells. *Science.* 297:1873–1877.

Pena, E., M.T. Berciano, R. Fernandez, J.L. Ojeda, and M. Lafarga. 2001. Neuronal body size correlates with the number of nucleoli and Cajal bodies, and with the organization of the splicing machinery in rat trigeminal ganglion neurons. *J. Comp. Neurol.* 430:250–263.

Rader, S.D., and C. Guthrie. 2002. A conserved Lsm-interaction motif in Prp24 required for efficient U4/U6 di-snRNP formation. *RNA.* 8:1378–1392.

Raghunathan, P.L., and C. Guthrie. 1998. A spliceosomal recycling factor that reanneals U4 and U6 small nuclear ribonucleoprotein particles. *Science.* 279: 857–860.

Raska, I., L.E. Andrade, R.L. Ochs, E.K. Chan, C.M. Chang, G. Roos, and E.M. Tan. 1991. Immunological and ultrastructural studies of the nuclear coiled body with autoimmune antibodies. *Exp. Cell Res.* 195:27–37.

Siegel, R.M., F.K. Chan, D.A. Zacharias, R. Swofford, K.L. Holmes, R.Y. Tsien, and M.J. Lenardo. 2000. Measurement of molecular interactions in living cells by fluorescence resonance energy transfer between variants of the green fluorescent protein. *Sci STKE*. 2000:PL1.

Sleeman, J.E., P. Ajuh, and A.I. Lamond. 2001. snRNP protein expression enhances the formation of Cajal bodies containing p80-coilin and SMN. *J. Cell Sci.* 114:4407–4419.

Sleeman, J.E., and A.I. Lamond. 1999. Newly assembled snRNPs associate with coiled bodies before speckles, suggesting a nuclear snRNP maturation pathway. *Curr. Biol.* 9:1065–1074.

Sleeman, J.E., L. Trinkle-Mulcahy, A.R. Prescott, S.C. Ogg, and A.I. Lamond. 2003. Cajal body proteins SMN and Coilin show differential dynamic behaviour in vivo. *J. Cell Sci.* 116:2039–2050.

Spector, D.L. 2001. Nuclear domains. *J. Cell Sci.* 114:2891–2893.

Staley, J.P., and C. Guthrie. 1998. Mechanical devices of the spliceosome: motors, clocks, springs, and things. *Cell.* 92:315–326.

Stanek, D., K. Koberna, A. Pliss, J. Malinsky, M. Masata, J. Vecerová, M.C. Risueño, and I. Raska. 2001. Non-isotopic mapping of ribosomal RNA synthesis and processing in the nucleolus. *Chromosoma.* 110:460–470.

Stanek, D., S.D. Rader, M. Klingauf, and K.M. Neugebauer. 2003. Targeting of U4/U6 small nuclear RNP assembly factor SART3/p110 to Cajal bodies. *J. Cell Biol.* 160:505–516.

Stevens, S.W., I. Barta, H.Y. Ge, R.E. Moore, M.K. Young, T.D. Lee, and J. Abelson. 2001. Biochemical and genetic analyses of the U5, U6, and U4/U6 x U5 small nuclear ribonucleoproteins from *Saccharomyces cerevisiae*. *RNA.* 7:1543–1553.

Tucker, K.E., M.T. Berciano, E.Y. Jacobs, D.F. LePage, K.B. Shpargel, J.J. Rossire, E.K. Chan, M. Lafarga, R.A. Conlon, and A.G. Matera. 2001. Residual Cajal bodies in coilin knockout mice fail to recruit Sm snRNPs and SMN, the spinal muscular atrophy gene product. *J. Cell Biol.* 154:293–307.

Verheggen, C., D.L. Lafontaine, D. Samarsky, J. Mouaikel, J.M. Blanchard, R. Bordonne, and E. Bertrand. 2002. Mammalian and yeast U3 snoRNPs are matured in specific and related nuclear compartments. *EMBO J.* 21:2736–2745.

Will, C.L., and R. Lührmann. 2001. Spliceosomal UsnRNP biogenesis, structure and function. *Curr. Opin. Cell Biol.* 13:290–301.

Yong, J., L. Wan, and G. Dreyfuss. 2004. Why do cells need an assembly machine for RNA-protein complexes? *Trends Cell Biol.* 14:226–232.